CHAPTER

1

INTRODUCTION

1.1 SEMICONDUCTOR TECHNOLOGY

The invention of silicon integrated circuits (IC) has brought a boom in the electronic industry. It has profoundly influenced the human civilization by the introduction of new technology applicable to several products like computer, telecommunication, automotive and consumer electronics, cellular phones, digital cameras, personal digital assistant and many more. For miniaturization of electronic products with enhanced performance and wider applications, electronic packaging technologies must be improved so as to meet future demand for electronic systems (Tummala *et al.*, 1999, Chen *et al.*, 2001). The electronic packaging which deals with storing more and more charge per unit surface area is, at present, the focus of an intense effort and a challenge for the microelectronic industries these days. It is an art of interconnection, protection and appropriate configuration of the system components with an intension of minimizing the profile and maximizing the performance of the IC and electronic system. The four core functions which it should fulfil are:

(i) to provide an electrical path to power the circuits;
(ii) to distribute signals onto and off the IC chip;
(iii) to remove the heat generated by the circuits;
(iv) to support and protect the chips from hostile environments.

The increase in transistor density of the semiconductor devices enhances demands for a corresponding increase in packaging interconnection density. A continuous stream of innovations and new developments in all aspects of electronic packaging materials, their processing and designs, reliability and testing, modeling and simulation are going on. The remaining driving forces including low cost, portability, high performance, multi-functionality and environmental friendliness also

impressed the technology revolutions of the last several decades. An integrated circuit may contain active, passive or embedded passive type of devices. An active device is a type of circuit component having the potential for controlling current. A circuit can be called electronic type, if it contains at least one active device like vacuum tubes, transistors, silicon controlled rectifiers, etc. Resistors, capacitors and inductors are a type of Passive devices. These devices are most prevalent in all electronic systems to provide impedance, current-to-voltage phase angle and energy storage. Unlike active components, passive devices are nonswitching and can't amplify; however, they can use their impedance in decreasing the signal current or voltage. Such properties are useful in many applications including voltage modification, current control or line termination. However, embedded passives, in which the passive components are embedded within the board itself, can be a better option for distinct parts by reducing substrate board space, cost, handling, assembly time and increasing productivity. Embedded passives can not only reduce the size and weight of the passives but can also have many other benefits such as increased reliability, improved electrical performance and reduced cost (Lu *et al.*, 2008). The benefits associated with embedded passives have driven a significant amount of research over the past few decades for this technology. However, embedded passive technology has still not been commercialized for electronic packages due to materials and process issues. Therefore, to enable embedded passive technology, it is necessary to develop materials that satisfy the requirements of fabrication as well as electrical and mechanical performances (Ulrich *et al., 2006*).

The rapid expansion of telecommunication systems and microelectronic Industry demands dielectric resonators (DRs) as primary components for designing filters and oscillators. Reducing their size is crucial for high-quality and low-cost devices. One of the most suitable ways of miniaturizing the filters and reducing their cost is to use any suitable ceramic materials with high dielectric constant and low dielectric loss. The essential characteristics required for those dielectric resonators are high dielectric constant (ε_r) for miniaturization, high quality-factor for selectivity. These dielectric resonators provide significant advantages regarding compactness, light weight, temperature stability and relatively low cost of the production of a variety of microwave devices such as band-selective filters and solid-state oscillators.

The recent technological advancements in microelectronics have created a great demand for interlayer dielectric materials with a very high dielectric constant which play a crucial role in the future generation of IC devices like VLSI/ULSI and high-speed IC packaging. Significant efforts have been distinctly manifested to develop some high dielectric constant materials for applications in microelectronic industries. Besides achieving high dielectric constant, other material properties such as high mechanical strength, high thermal and environmental stability, low thermal expansion, low current leakage, low moisture absorption, high corrosion resistant, etc., are of equal importance (Kotecki *et al.*, 1997; Moulson *et al.*, 2003). Many chemical and physical strategies have been employed to get desired dielectric materials with high performance. The ultimate goal of such efforts is to miniaturize a variety of electronic devices with the same time upgrading their quality and performance. The size of the ceramic can be reduced by enhancing its dielectric constant because the size of the resonator is inversely proportional to square root of the dielectric constant of the material. As the size of integrated circuits continue to decrease with simultaneous increase in speed, the requirement for higher dielectric constant materials increases significantly. The challenges of dielectric materials will become even more severe as the industry approaches nano-meter generation and traditional ceramic-filled composites will be replaced gradually with novel nano-electronic materials. A focus on both improving multifunctional properties and better understanding the processes is required to produce these new materials (Ulrich *et al.*, 2006).

1.2 DIELECTRICS: OPTIONS FOR EMBEDDED CAPACITORS

High dielectric materials find application in embedded capacitors. To date, not a single perfect dielectric material has yet been identified for embedded capacitor applications because they all compromise on certain issues including electrical and mechanical performance or processing constraints. However, a very wide range of primary candidates are potentially available. The Perovskite oxides family are well known for their ability to produce high dielectric constant.

1.2.1 Dielectric Ceramic Materials: An Overview

Dielectric characteristics of ceramic materials are of great interest in the electronic ceramic industry. The ceramic dielectrics can be used either as an electrical insulator or in terms of capacitive elements in electronic circuits. The storage property of high dielectric materials is quite useful for capacitors and hence finds applications in virtually any electricity-driven devices (Lines and Glass, 1977; Nair and Bhalla, 1998). Modified $CaTiO_3$ and $SrTiO_3$ ceramics find use in barrier layer capacitors (Waku, 1969). Some ceramic capacitors of different dimensions are shown in Fig. 1.1. Recent technological developments in wireless telecommunication are based in parts on the fabrication of superior dielectrics (Reaney and Ubic, 2000). Many capacitor formulations resemble $BaTiO_3$ [BT], $PbMg_{1/3}Nb_{2/3}O_{3-X}$ [PMN], $PbZn_{1/3}Nb_{2/3}O_{3-x}$ [PZN] and $Pb_{1-x}La_x(Zr_{1-y}Ti_y)O_3$ [PLZT] dielectric material which crystallizes with the perovskite structure.

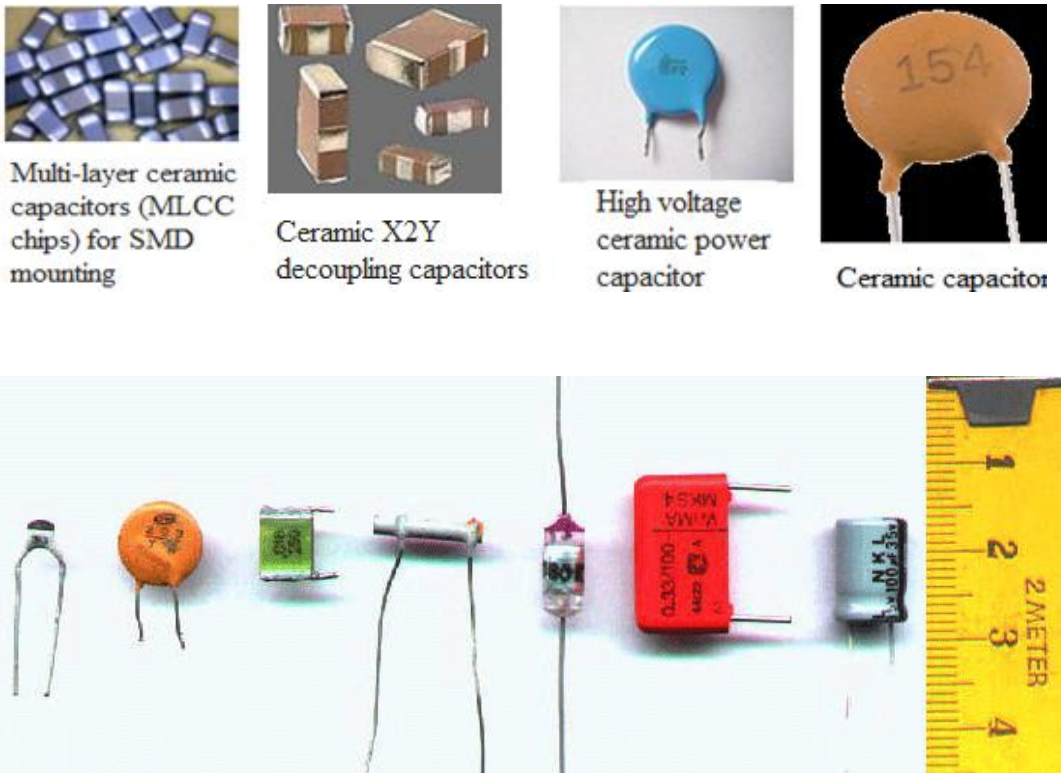

Figure 1.1: Some Ceramic capacitors

Dielectrics are the materials with high electrical resistivity. It is a poor electrical conductor but an active supporter of electrostatic fields. If the current between the two opposite poles is kept to a minimum and the electrostatic flux lines are not interrupted, maximum energy can be stored by an electrostatic field. Thus, a material can be classified as 'dielectric' only if it has an ability to store energy when an external electric field is applied.

A good dielectric is, of course, necessarily a good insulator, but the converse is by no means true. The dielectrics can be polarized by the application of an external electrical field. When a dielectric material is placed in an electric field, electric charges do not flow through it; rather get shifted from their average equilibrium position causing polarization. The extent of polarization originated is described by a dimensionless quantity called the dielectric constant (represented by ε). It describes the ability of any material to polarize in response to the field and thereby reduce the total electric field inside the material (Chen *et al.*, 2001).

Dielectric materials are efficient in storage of electrical energy in the form of charge separation when the electron distribution around the constituent atoms or molecules is polarized by an external electric field. But in an applied AC field, the dielectric response of an ideal dielectric material lags behind its value in a DC field. In this situation, the dielectric constant) of material becomes a complex quantity, ε^* which can be represented by:

$$\varepsilon^* = \varepsilon^{/} - i\varepsilon^{//} \tag{1.1}$$

where $\varepsilon^{/}$ and $\varepsilon^{//}$ are the real and imaginary components of ε and i =√-1. The magnitude of $\varepsilon^{/}$ and $\varepsilon^{//}$ both depend on the frequency of the applied field. The real part of dielectric constant of material is given by:

$$\varepsilon^{/} = \varepsilon_o \varepsilon_r \tag{1.2}$$

where ε_o is the permittivity or dielectric constant of free space ($\varepsilon_o = 8.854 \times 10^{-12}$ F/m) and ε_r the relative permittivity or dielectric constant of the material. The dielectric constant (ε_r) may be defined as a measurement of the ability of the material to store charge relative to vacuum. The imaginary part of the permittivity ($\varepsilon^{//}$) is also called as

dielectric loss. It is desired to minimize the dielectric loss for an energy storage device like a capacitor.

The embedded capacitors are fabricated into a parallel plate configuration, where the capacitance is calculated by the following equation

$$C=\varepsilon_o\varepsilon_r A/d \qquad (1.3)$$

where C is the capacitance (F), ε_r is the dielectric constant, A is the electrode area and d is the thickness of the dielectric layer (Fig. 1.2). In terms of a parallel-plate capacitor dielectric constant (ε_r) is a factor by which its capacitance can be increased by inserting a dielectric material in place of vacuum. It is clear that the larger is the dielectric constant, larger the capacitance which can be realized in a given space. Therefore, materials of high dielectric constant are favoured in the practical design of embedded capacitors for miniaturization.

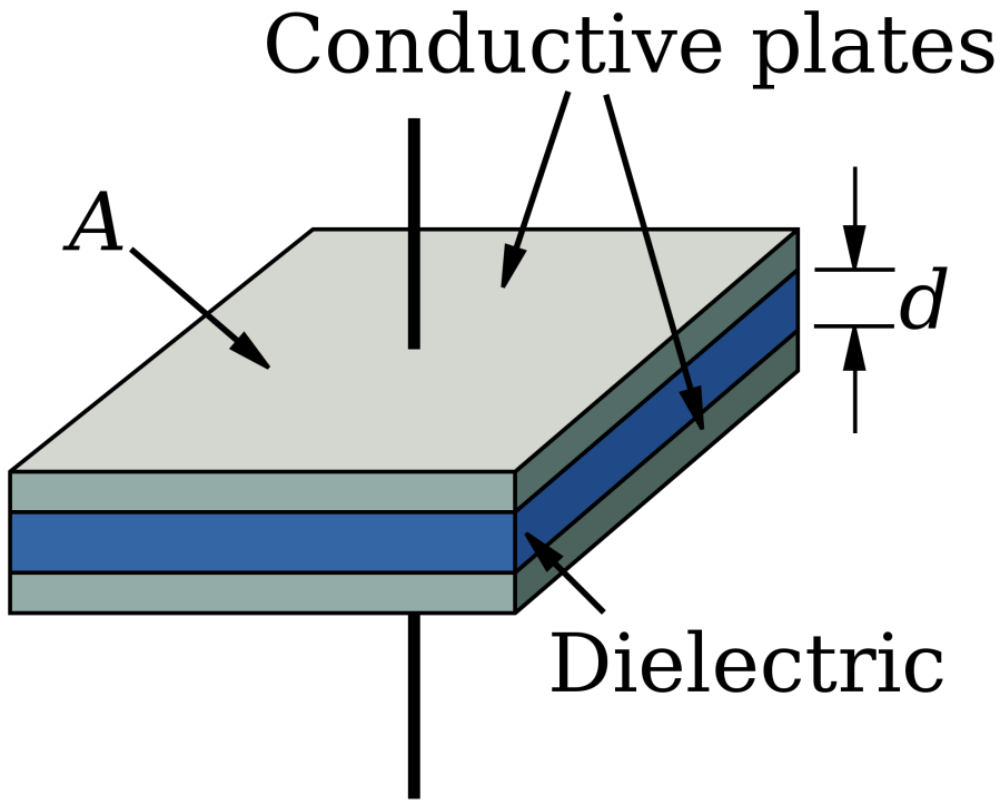

Figure 1.2: A parallel plate capacitor with an inserted dielectric

1.2.1.1 Dielectric Loss

With the change in polarisation in a material due to an applied electric field, some field energy is dissipated either due to charge migration, so called conduction process or due to its conversion into thermal energy (in case of molecular vibration). The measurement of such type of energy dissipation in the dielectric during an AC field application is called dielectric loss.

Basically, the energy loss in a dielectric material result from three processes (Kingery *et al.*, 1991)

i) Long range electronic or ionic migration losses (i.e. DC conductivity)

ii) Relaxation losses for dipole reorientation due to ionic jump and

iii) Ion vibration and deformation losses.

Dielectric loss, being a material property, does not depend on the geometry of capacitor. The dielectric loss is expressed in terms of the loss tangent (tan δ) or dissipation factor (D_f). A mathematically expression of tan δ is given by the following equation

$$\tan \delta = \frac{\varepsilon''}{\varepsilon'} + \frac{\sigma}{2\pi f \varepsilon'} \quad (1.4)$$

where ε' and ε" are the real and imaginary part of the dielectric permittivity, σ is the electrical conductivity of the materials and f is the frequency. The dielectric loss of the dielectric material is an overall result of distortional, dipolar, interfacial and conduction loss. The distortional loss is originates due to electronic and ionic polarizations. The interfacial loss originates from the excessively polarized interface induced by the fillers and precisely the movement or rotation of the atoms or molecules in an alternating electric field. The conduction loss arises due to the dc electrical conductivity of the materials, representing the flow of actual charge through the dielectric materials (Lu *et al.*, 2008).

The loss factor is the primary criterion for the usefulness of a dielectric as an insulator. Therefore, a small dielectric loss is preferred to reduce the energy dissipation and signal losses, particularly for high-frequency applications. A

dissipation factor under 0.1% is considered to be quite small and 5% as very high. A very low dissipation factor is desired for radio frequency (RF) applications to avoid signal losses, but much higher values can be tolerated for energy storage applications such as decoupling. For use of a dielectric as an insulator, it is desirable to have a low dielectric loss and low dielectric constant but as a capacitor, in the smallest physical space, high dielectric constant and low dissipation factor is desirable.

1.2.1.2 Dielectric Strength

Dielectric strength is defined as the electric field which is just sufficient to initiate a breakdown of the dielectric without physical degradation of its insulating properties. It depends on several factors like the composition of material as well its homogeneity and microstructural features (like porosity, cracks, flaws, secondary phases). Few parameters such as electrode configuration, specimen thickness, temperature, time, frequency, stress mode (DC, AC or pulsed) humidity and heat transfer conditions also significantly influence the dielectric strength (Kingery *et al.*, 1991).

1.2.1.3 Polarization

The response of dielectric material in an electric field is defined by a parameter called polarization, which is the dipole moment per unit volume of the material. There are several mechanisms associated with polarization. These includes electronic, atomic or ionic, molecular or dipole, orientation and interfacial or space-charge polarization. Under an applied electric field, each of these mechanisms causes a displacement of charge resulting in polarization in the direction of the field. This effect of electric field on each mechanism has been schematically shown in Fig. 1.3.

For a given dielectric material, the net polarization (*P)*, is the sum of the contributions from each mechanism.

$$\text{i.e.} \quad P = P_{electronic} + P_{ionic} + P_{molecular} + P_{\text{interfacial}} \tag{1.5}$$

Electronic polarization occurs in neutral atoms. It occurs due to displacement of positive nucleus with respect to electrons around it under the influence of an electric field. This creates an induced dipole moment. This effect is universal and its

magnitude is usually very small in comparison to other polarizations. Electronic polarization occurs at very high frequencies around 10^{15} Hz and results into a low dielectric constant value.

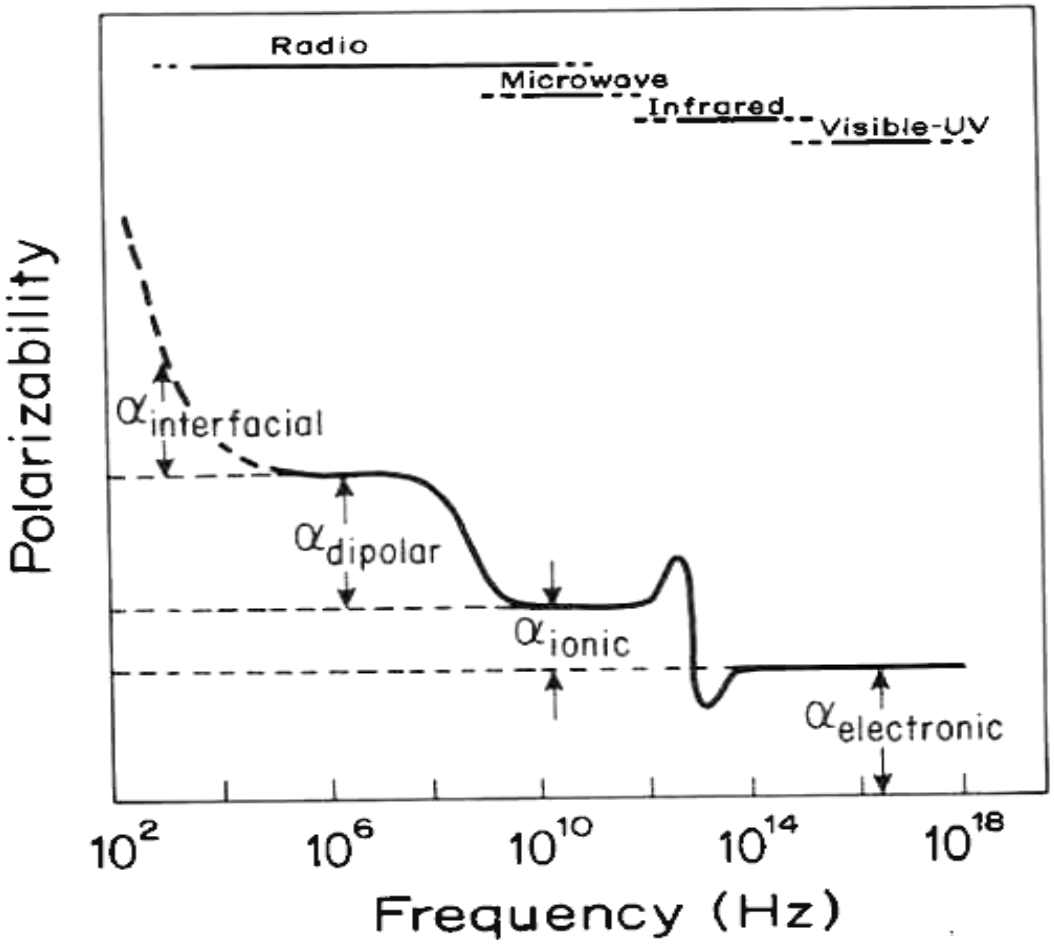

Figure 1.3: Typical response of the total polarizability of a crystal as a function of crystal as a function of electric field frequency (Lasaga and Cygan, 1982).

In atomic or ionic polarization, stretching of chemical bonds between dissimilar atoms in a molecule creates a change in dipole moment. When an electric field is applied, the electron cloud shifts towards the more electronegative atoms resulting into a permanent dipole. These dipoles get aligned creating thereby an enhanced capacitance which is also affected by the microstructure of the ceramic material, lattice flexibility and its composition. The magnitude of atomic polarization is as small as one-tenth of electronic polarization. It cannot occur at very high

frequencies because of the much slower movement of heavy nuclei compared to electrons.

Molecular or dipolar polarization occurs in substances containing permanent dipole moment resulting from unequal sharing of electrons by atoms of a molecule and the rotations of the permanent dipoles to align with the external electric field. This type of polarization occurs in the frequency range 10^{11} to 10^{12} Hz.

Space charge or interfacial polarization occurs in multi-component heterogeneous systems. The charge carriers get accelerated when an electric filed is applied. It can migrate an appreciable distance through the dielectric unless they are impeded and get trapped at the physical boundaries. Grain boundary and interfaces between different components in a ceramic material are the main physical obstacles. This building up of charge induces polarization in the material. This type of polarization occurs around 10^{-3} to 10^{3} Hz.

In an alternating electric field, the different polarization processes relax with increasing frequency. The space charge polarization relaxes at the lowest frequency while the electronic polarization at the highest.

Ideally, the dielectric constant should be a constant irrespective of the change in frequency, temperature, voltage and time. However, since each polarization has a characteristic relaxation frequency the dielectric value of most of the materials exhibits its dependence on the frequency. The dielectric values can also vary with temperature, bias, impurity and crystal structure to a different extent according to materials types.

1.2.1.4 Debye Relations

Debye relations give the complex dielectric constant for any polarisation relaxation process:

$$\varepsilon^{*} = \varepsilon_{\infty} + \frac{(\varepsilon_{s} - \varepsilon_{\infty})}{(1 + i\varpi\tau)} \tag{1.6}$$

where ε_s represent the static dielectric constant (i.e. dielectric constant at very low frequency), ε_∞ is the dielectric constant at very high frequency, $\omega = 2\pi f$ is the angular frequency, f is the frequency in cycles per second, τ is the relaxation time and $i = \sqrt{-1}$, an imaginary number. The complex quantity, ε^* can be separated into the real and imaginary parts as

$$\varepsilon^{/} = \varepsilon_\infty + \frac{\left(\varepsilon_s - \varepsilon_\infty\right)}{\left(1 + \varpi^2 \tau^2\right)} \tag{1.7}$$

$$\varepsilon^{//} = \frac{\left(\varepsilon_s - \varepsilon_\infty\right)\varpi\tau}{\left(1 + \varpi^2 \tau^2\right)} \tag{1.8}$$

The dielectric loss (tan δ) can be equated as

$$\tan\delta = \frac{\varepsilon_r^{//}}{\varepsilon_r^{/}} = \frac{\left(\varepsilon_s - \varepsilon_\infty\right)\varpi\tau}{\left(\varepsilon_s + \varepsilon_\infty \varpi^2 \tau^2\right)} \tag{1.9}$$

These equations are known as Debye equations. The Debye curves for dielectric dispersion $\varepsilon^{/}$ and loss (absorption) $\varepsilon^{//}$ are symmetric about $\omega\tau = 1$. These plots are shown in Fig. 1.4. The maxima of the absorption curve and midpoint of the dispersion curve occur at a frequency given by $\omega_{max} = 1/\tau$ and the full width at half maxima (FWHM) of the absorption curve is approximately 1.14 decades in frequency for a single value of relaxation time.

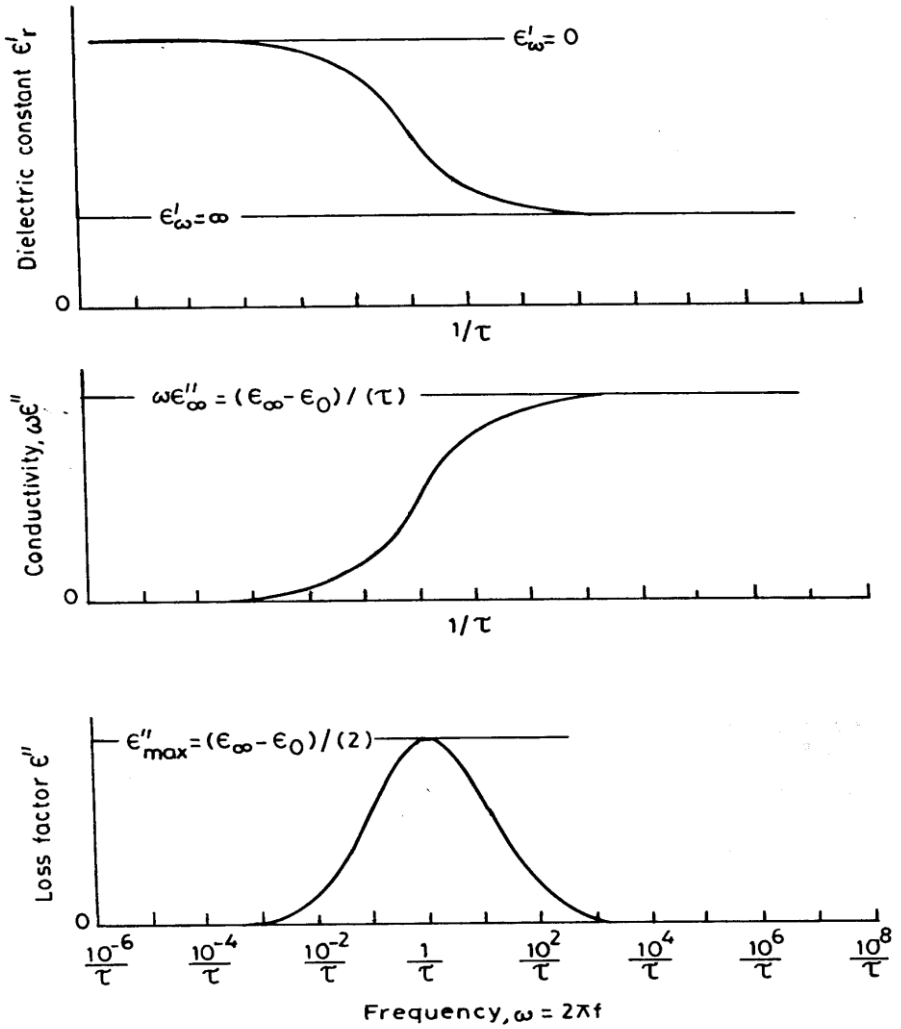

Figure 1.4: Relaxation spectra of ε, conductivity and loss factor for a simple relaxation process with a single relaxation time.

1.2.2 Conduction Losses and Degradation

Oxygen vacancies are important in the high-temperature region. The rapid increase of dissipation factor is caused by free carrier conductivity and the concentration of free carriers depends on the process and extent of doping as well as on temperature. The loss factor (tan δ) is inversely proportional to frequency in this temperature range.

Polycrystalline titanates get reduced at a temperature used in firing ceramic capacitors. On cooling, rapid re-oxidation occurs above 1100 °C but stops at some temperature between 600 and 900 °C. As a consequence, the outside of the sample and

to some extent, the outside of each grain is well oxidized, but the interior of the grains remains oxygen deficient. Oxygen vacancies carry an effective charge of +2e, which is neutralized by 3d electrons on the titanium atoms, forming two Ti^{3+} ions for every oxygen vacancy. At low temperatures, the oxygen vacancies and Ti^{3+} ions are bound by a small energy of 0.1-0.2 eV which is sufficiently large so that only a few of defects are separated. Electrons associated with the unattached Ti^{3+} ions are responsible for conduction making use of the narrow 3d conduction band. Alternatively the conduction process can be described as electron hopping via $Ti^{3+} \leftrightarrow Ti^{4+} + e^-$ transfer. Unattached oxygen vacancies also contribute to the conductivity bur their mobility is much smaller than that of electrons (Newnham, 1983). Neutralized bound defects do not participate directly in the conduction process but experience a torque tending to align the dipole moment with the applied field which in turn creates dielectric polarization and dielectric loss.

1.3 PEROVSKITE OXIDES: A GENERAL OVERVIEW

Perovskite is a naturally occurring mineral with composition $CaTiO_3$. It forms a large family of crystalline ceramics with the general formula ABO_3. An ideal perovskite is a mixed transition metal oxide where A is an alkaline earth ion, B is the transition metal ion and O is the oxygen anion. In a cubic unit cell of perovskite oxides, cation A occupies the eight corner positions, cation B occupies the body centre position and oxygen anion occupies the six face centre positions (Fig.1.5a). It consists of corner sharing [BO_6] octahedra with cation A occupying the 12-fold coordination site formed in the middle of the cube of eight such octahedral, as shown in (Fig.1.5b) (Polla *et al.*, 1998). In terms of close packing, an alternate BO_6 and A-O layers stacked over one another in perovskite in <001> direction while AO_3 layers are staked over one another with B cations, occupying the octahedral holes surrounded by oxygen ions.

During distortion, cation A causes a tilting of [BO_6] octahedral to optimize A-O bonding. The distortion of [BO_6] octahedra due to temperature changes or other stress effects may cause from cubic to tetragonal, rhombohedral or orthorhombic structures. Distorted perovskites have reduced symmetry, which is quite important for their magnetic and electric properties.

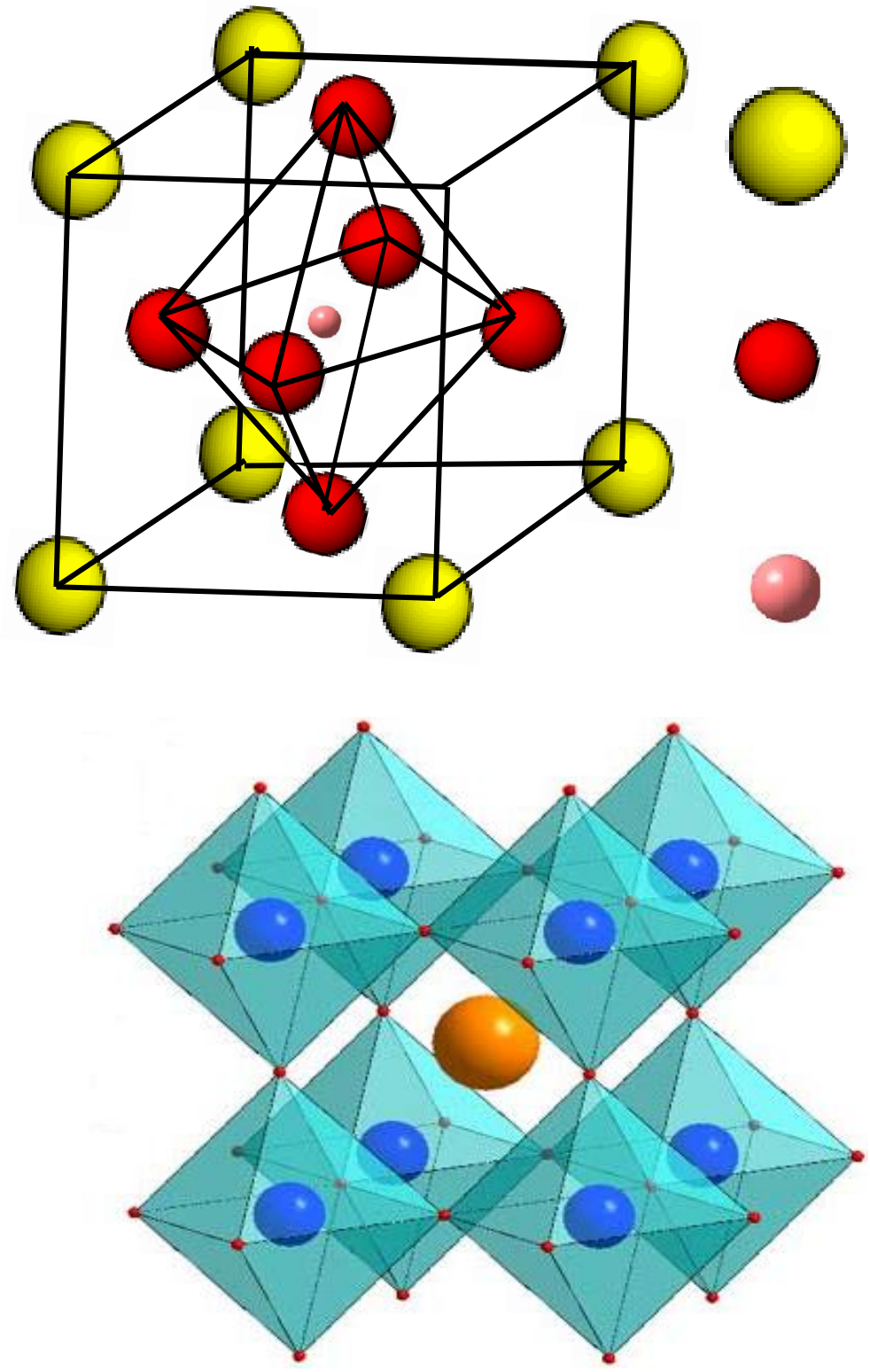

Figure 1.5 (a) A unit cell of ABO_3 type cubic perovskite oxide

(b) Corner sharing of $[BO_6]$ octahedra in perovskite structure

The three main factors, being identified as a plausible reason for the distortion in perovskite structure are: Size effect of cation A and B, deviation from an ideal composition and the Jahn-Tellar effect (Chen *et al.*, 2001). It is very hard to assign a single effect as a reason for distortion in a specific perovskite oxide.

(i) Size Effects

Perovskite structure is known to be very flexible depending upon the variation of cation A and B. It leads to a large number of known compounds with perovskite or its related structure. Goldschmidt (1926) proposed the following empirical rules for the stability of ABO_3 type perovskites:

(i) An ion has a radius that does not vary to more than a few percent in the different structures in which it occurs.

(ii) For a set of cation and surrounding anions, all the anions must touch the cation.

According to Goldschmidt (1926), the geometrical requirements for the formation of perovskite structure is that the ionic radii r_A, r_B and r_0 of cations A, B and anions O respectively, must satisfy the following relation:

$$t = \frac{(r_A + r_O)}{\sqrt{2}(r_B + r_O)} \qquad (1.10)$$

where t is the tolerance factor, which describes the range of relative sizes for which the perovskite structure is stable. If cation A is smaller in size and cation B is larger in size than the ideal structure, then t becomes smaller than 1. As a result, the $[BO_6]$ octahedra will tilt to fill the space and strain produced will disturb its regular cubic geometry.

In general, the perovskite structure occurs only within the range $0.75 < t < 1$, which is given solely based on geometric considerations (Maiti *et al*, 2007). Limiting values for the tolerance factor is determined experimentally. For example, the ideal perovskite structure can be found in high-temperature phases or compounds with

more ionic A-O bonds. The structure will be cubic if $0.95 < t \leq 1.0$ and orthorhombic if $0.75 \leq t \leq 0.9$. An ideal example of cubic perovskite is $SrTiO_3$, with $t = 1.00$, $r_A = 1.44$ Å, $r_B = 0.605$ Å. A lower value of t will reduce the crystal symmetry. For example $GdFeO_3$ with $t = 0.81$ is orthorhombic ($r_A = 1.107$ Å, $r_B = 0.78$ Å) (Bhalla et al, 2000). If t is larger than 1, i.e. for set of cation A (large) and cation B (small), then perovskite adopts a stable hexagonal geometry. For example $BaNiO_3$, with $t = 1.13$, $r_A = 1.61$ Å, $r_B = 0.48$ Å. In fact, compounds having tolerance factor in the range $0.75 \leq t \leq 0.95$ are non-ferroelectric with distorted structure while those with $t \geq 1.0$ are ferroelectric (Wood *et al.*, 1951; Keith *et al.*, 1954; Roth *et al.*, 1957). If $t < 0.75$, the compound does not crystallize in perovskite structure rather adopts a hexagonal ilmenite structure ($FeTiO_3$).

However, perovskites are not truly ionic compounds; the tolerance factor can only give an approximate crystal structure.

(ii) Compositional Effects

A variety of stable perovskite can be obtained by considering a compatible range of size of cations A and B and its valency. In close packing of perovskites, the presence of interstitial ions appears unlikely; however, substantial concentration of A-site vacancies can be tolerated. A mixture of perovskite or non-perovskite structure crystallizes out for substantial concentration of B-site vacancies for e.g., in $SrFeO_x$ ($2.5 \leq x \leq 3$), as valency of Fe ions can be changed, according to oxidising or reducing environment, oxygen content can adjusted between 2.5 to 3 (Jiang *et al.*, 1998). But in case of $SrFeO_{2.875}$, some Fe ions can be assigned to Fe^{3+} and Fe^{4+}, square pyramids of FeO_5 are formed.

(iii) Jahn-Teller Effects

Jahn-Teller Effects is an important factor to lower down the symmetry of perovskite, especially if it contains ions with an odd number of electrons in the e_g-orbital. It includes perovskite compounds ABO_3 where cation B is either Mn^{3+}, Cr^{2+}, Fe^{4+}etc. in high spin state or Ni^{3+}, Cu^{2+} etc. in low spin state. For example in $LnMnO_3$ (Ln = La, Pr or Nd), with Mn^{3+} ($3d^4$) in the octahedral coordination field results into elongation of the MnO_6 polyhedron. It means the perovskite possesses high extent of

structural flexibility. A large number of different but closely related structures can be obtained with the general chemistry of ABO_3 and the other requirements. Doping with a specific ion/composition produces new compounds and thus provides a path to chemically tune structural and physical properties. Doping must maintain the charge balance in perovskites, keeping sizes of corresponding ions with the range for a particular coordination number.

In brief, the following points regarding geometry and electronic configuration are important:

a) The r_A/ r_O should be approximately 1 or slightly higher.

b) The tolerance factor for the perovskite structure using Pauling corrected radii should be approximately 1.05.

c) The ionization potential of B should be 40 kJ/mol or higher.

d) The electronegativity of O^{2-} ion should be 2.5 or greater.

1.3.1 Different Types of Perovskite Oxides

Perovskite oxides can be categorized into three different types depending upon valency of cations A and B in ABO_3 perovskites (Yakel *et al.*, 1955; Galasso *et al.*, 1969). *For* stoichiometric compounds, the combination of A^{m+} and B^{n+} are such that they satisfy the charge-neutrality criteria given by (m + n) = 6 i.e., sum of the valencies of the cations must be equal to that of anions. To meet this criterion, the cation A may be chosen from the first, second and third group of the Periodic Table and cation B from the fifth, fourth and third group of the Periodic Table, respectively (Wainer and Wenworth, 1952). No tetravalent or pentavalent ion on A-site has been known to stabilize the perovskite oxides. Therefore, only three categories of perovskite oxides exist, which are as follows:

(i) **$A^{1+}B^{5+}O_3$ type:** The cation A belong to the first group and cation B belong to the fifth group of the periodic table. $LiNbO_3$, $KNbO_3$, $AgNbO_3$, $NaTaO_3$, $AgTaO_3$, $KTaO_3$ etc. are some of the examples of this type of perovskite. Most

of such compounds of this type are either ferroelectric or anti-ferroelectric (Matthias, 1949).

(ii) $\mathbf{A^{2+}B^{4+}O_3}$ **type**: The cation A belong to the second group like Ca, Sr or Ba and cation B belong to the fourth group like Ti, Zr and Zn of the periodic table. Among these perovskites, the most widely studied materials are $ATiO_3$ where A = Ba, Sr, Ca and Pb. These materials are used as dielectric and piezoelectric materials. These are also used as thermistors and as humidity sensors (Jaffe *et al.*, 1971; Hill and Tuller., 1986; Funayama *et al.*, 1989; Gerblinger and Meixner, 1991).

(iii) $\mathbf{A^{3+}B^{3+}O_3}$ **type**: The cation A and B both belong to the third group of the Periodic Table. The compounds belonging to this category have a rare earth metal or Yttrium ion on A-site and a trivalent transition metal ion on B-site. Such compounds have technical application as functional materials in many fields because of their unusual properties such as mixed conductivity by both ions and electrons or through migration of holes (Goodenough, 1974). Such materials can be used in solid electrolyte fuel cells (Yamamoto *et al.*, 1987; Minh et al., 1993) as an electrode materials, in oxygen sensors (Inoue *et al.*,1990; Alcock *et al.*, 1992; Shuk *et al.*, 1993) and as humidity sensors (Shimizu *et al.*, 1985; Lukaszewicz 1991).

Out of these perovskite oxides, $\mathbf{A^{2+}B^{4+}O_3}$ **type** and $\mathbf{A^{3+}B^{3+}O_3}$ **type** are of prime importance.

1.3.2 Substitution in Perovskites

Oxides with the perovskite structure are well known for their high dielectric constants (ε) which led to a large number of technological applications. The perovskites are technically important even in undoped form, however, doping with different cations modify their properties (Patterson *et al.*, 2005; Prakash *et al.*, 2008; Li *et al.*, 2006; Shao *et al.*, 2007; Rai *et al.*, 2009; Mandal *et al.*, 2009). The perovskite oxides in pure state i.e. in undoped form have only limited applications. Compositional modification in perovskites oxides is useful in changing their properties. As perovskites have close packed structure, interstitial substitution is

difficult to make. There is a lot of flexibility of substitution on A or B site of perovskite ABO_3. The following factors affect the substitution modification:

a) **Size**: If the size of two ions differs by less than 15%, the condition is favourable.

b) **Chemical Reactivity:** The greater the chemical reactivity of the two crystalline materials, the more restricted will be the solid solubility.

c) **Structure**: For complete solid solubility the two solids must have the same crystal structure.

d) **Valence**: If the added ion has a valency different from the host ion, substitution is limited.

The various types of substitution in perovskite oxides are as follows:

(i) Independent isovalent substitutions
(ii) Independent heterovalent substitutions
(iii) Valence compensated substitutions

1.3.2.1 Independent Isovalent Substitutions

In isovalent substitutions, the valency of substituting ions is the same as that of the host cations at A or B site. Substitutions may be on A-site, B-site or simultaneously on both A and B sites, In $BaTiO_3$, substitutions of Ca^{2+}, Sr^{2+} or Pb^{2+} are isovalent substitution at A site while substitution of Ti^{4+} by Zr^{4+}, Sn^{4+} of Hf^{4+} are isovalent substitution at B site. Isovalent substitution influences the transition temperature beside other properties and may increases peak value of dielectric constant.

1.3.2.2 Independent Heterovalent Substitutions

In heterovalent substitution the substituent and substituted ions have different valencies. These substitutions also may be either on A or B site. Heterovalent substitutions are of two types:

(i) **Accepter substitution**: An acceptor ion has lower valency than that of the host ion it replaces and the resulting negatively charged impurity centre can be compensated by oxygen vacancy, donor impurity or holes. The substitution of Na^{+} on Ba^{2+} and Co^{3+} on Ti^{4+} site in $BaTiO_3$ is very common.

(ii) **Donor substitution**: In this case, the substitution impurity ion has higher valency than that of host ion on A or B site. The impurity thus bears an effective positive charge, e.g. La^{3+} or Y^{3+} on Ba^{2+} (Zhi *et al.*, 1999) and Nb^{5+} on Ti^{4+} site in $BaTiO_3$ separately. Charge compensation in this case is achieved either through electron or cations vacancies on A or B sub-lattice (Jaffe *et al.*, 1971; Newnham *et al.*, 1983).

1.3.2.3 Valence Compensated Substitutions

In this case simultaneous substitutions of a combination of ions at A and B sub-lattice sites are such that total electric charge neutrality in the crystal is maintained internally. Simultaneous valence compensated substitutions are of two types:

(i) Simultaneous substitution of isovalent ions on A and B sub-lattice site for e.g. $Pb_{1-x}Ba_xTi_{1-x}Sn_xO_3$

(ii) Simultaneous substitution of heterovalent ions on A and B sub-lattice sites so that the charge balance is maintained internally without requiring the change in the oxidation state of an ion or creating vacancies in A, B or O sub-lattices such that $M_{1-x}La_xTi_{1-x}M'_xO_3$ such M = $Ca^{2+,}$ $Sr^{2+,}$ Ba^{2+} or Pb^{2+} and M$^{/}$ = $Co^{3+,}$ $Ni^{2+,}$ Fe^{3+} etc. (Prasad *et al.*, 1988; Parkash *et al.*,1990; Tewari *et al.*, 1990; Christopher *et al.*, 1988). Such solid solutions are known as valence compensated solid solutions (VCSS).). e.g., La^{3+} ion on Ba^{2+} site and Co^{3+} on Ti^{4+} site substituted simultaneously in $BaTiO_3$: $Ba_{1-x}La_xTi_{1-x}Co_xO_3$. In this case there is a little chance of defect creation. In the system $Ba_{1-x}La_xTi_{1-x}Co_xO_3$, ferroelectric to paraelectric transition is observed in the composition range $x \leq 0.05$ (Parkash *et al.*, 1991).

1.3.3 Different Synthesis Routes for Preparation of Perovskites

The perovskite oxides are generally synthesized by conventional solid-state route which is also called as a dry route. In this route, oxides of various cations are

mixed in stoichiometric ratio and ground to fine powder using a mortar-pestle using a suitable liquid (acetone or ethanol). Dried mixed powder is calcined at a particular temperature for a certain period of time and ground again in to fine powder. An optimum amount of a suitable binder (PVA) is added to the powder and mixed uniformly and then it is pressed in to a suitable shape. The resulting product is first heated slowly to a particular temperature to burn off the binder and then the temperature of the sample is increased to a particular value and maintained at this value for certain duration for annealing. After annealing, the sample is cooled at a controlled rate of cooling. The final resulting product is achieved by diffusion of metal ions at high temperature. This procedure requires tedious work, relatively long reaction time and high temperature condition. In addition, some other secondary phases also appear during synthesis because of limited atomic diffusion through micrometer sized grains. Therefore, repeated grinding, mixing and annealing is required at high temperature to attain chemical homogeneity. This does not lead to chemical homogeneity at micro level in the end product. On the other hand, the wet chemical methods provide atomic level mixing of individual components and result in the formation of nanocrystalline materials at much lower temperature compared to solid state reactions. There are many chemical methods, such as, sol-gel, co-precipitation, precursor solution technique and hydrothermal process (Jha *et al.*, 2003) which have been used for the synthesis of the ceramics.

Pechini's method is used for the synthesis of titanates and niobates for the capacitor industry. The modified Pechini methods, known as the citrate gel process or the amorphous citrate gel process are used for the preparation of a wide variety of ceramic oxide powders. (Pechini *et al.*, 1967) The technique involves mixing of solutions of a metal precursor and an organic polyfunctional acid possessing at least one hydroxyl and one carboxylic acid group such as citric acid, glycine, tartaric acid and glycerol which results in complexation of the metal by the polycarboxylic acid. The solutions are heated to evaporate water and on its complete removal a highly viscous resin is formed. The resin is then heated to decompose the organic constituents, ground and finally calcined to produce the powder.

Glycine gel nitrate process is one of the combustion methods for the synthesis of ceramic powders. A highly viscous mass formed by evaporation of a solution of

metal nitrates and glycine is ignited to produce the powder (Chick *et al.*, 1990). Glycine is a complexing agent and prevents the precipitation of the metal ions as the water is evaporated. It can form complex with cation at both the carboxylic end and the amino group end as illustrated in Fig.1.6. Glycine also serves another important function that it provides a fuel for the ignition step of the process as it is oxidized by the nitrate ions. The reactions occurring during ignition are highly explosive and extreme care must be exercised during this step. Normally, only small quantities should be ignited at a time. Under well controlled conditions, a loose mass of very fine crystalline powder is obtained after ignition and hence in contrast to the Pechini method, no grinding is required. The very fine size and crystalline nature of the powder are believed to be direct consequence of short exposure to high temperature during the ignition step. Glycine gel nitrate process, therefore, offers a relatively inexpensive route for the synthesis of very fine chemically homogeneous powder. It has been used for the synthesis of simple oxides as well as complex oxides e.g. manganites, chromites, ferrites and oxide superconductors.

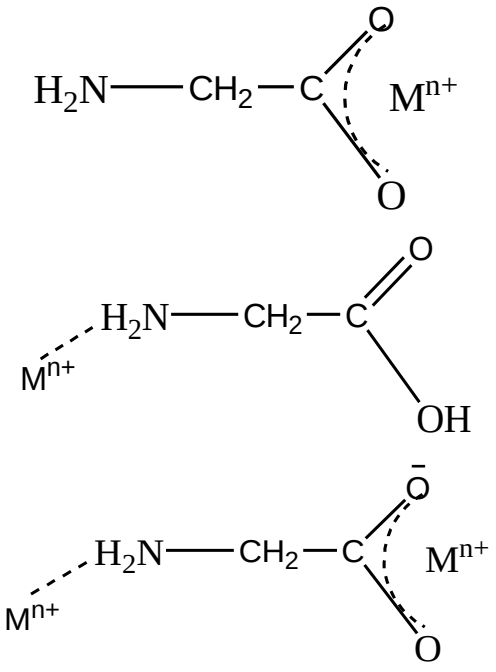

Figure 1.6: Zwitter ion of glycine molecule co-ordinated with M^{n+}

1.3.4 Some Important Perovskites Exhibiting High Dielectric Constant

A large number of ABO_3 type perovskites such as $BaTiO_3$, $CaTiO_3$, $SrTiO_3$ etc. possess high dielectric constant.

1.3.4.1 Barium Titanate ($BaTiO_3$)

$BaTiO_3$ is a ferroelectric perovskite exhibiting a high value of dielectric constant (200-3000) at room temperature. In $BaTiO_3$, both barium and oxygen ions have radii of about 1.40 Å and occupy corner and face centred cubic array, respectively. The octahedrally coordinated titanium ions, located at the body centre of a perovskite unit cell, are the active ions promoting ferroelectricity in crystal. With increasing temperature, $BaTiO_3$ shows five crystalline phases: rhombohedral, orthorhombic, tetragonal, cubic and hexagonal. Among these, tetragonal phase is the most stable at room temperature. $BaTiO_3$ undergoes three ferroelectric phase transitions (shown in Fig. 1.7) which are interchangeable in nature involving atomic movements of 0.10 Å or less.

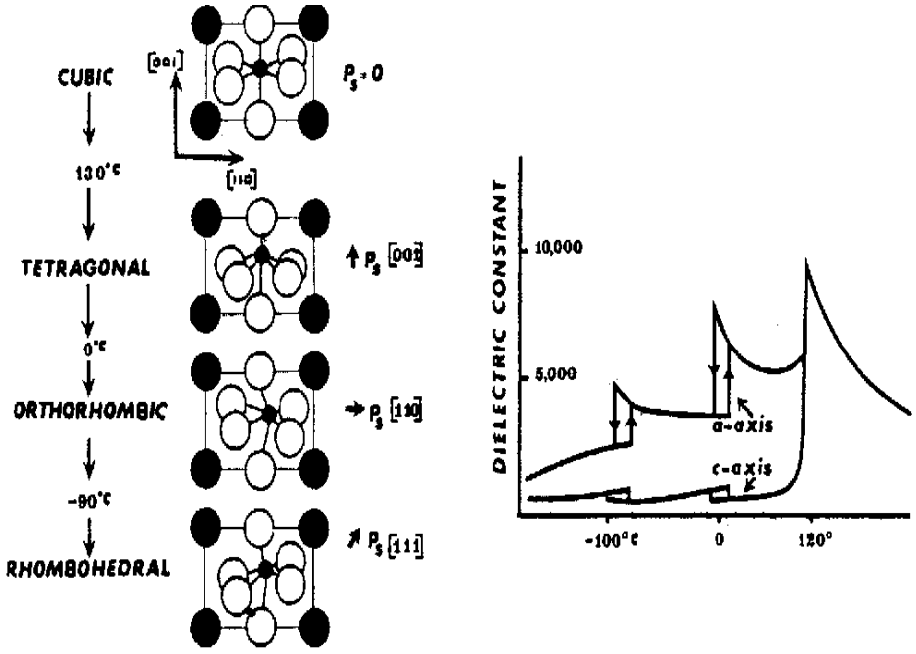

Figure 1.7: Structural changes occurring at the three ferroelectric phase transformations in $BaTiO_3$ (Newnham, 1983).

The direction of spontaneous polarization changes from one ferroelectric phase to another. But at temperature above 1460 °C, it transforms in to non-ferroelectric hexagonal form (Kay *et al.*, 1949). Below this temperature, it exists in the cubic form, which is paraelectric. At room temperature $BaTiO_3$ is tetragonal with axial ratio c/a ≈ 1.012 (Jaffe *et al.*, 1971). The polymorphic phase transitions at lower temperatures are found to occur as:

$$\text{Rhombohedral} \xleftrightarrow{-90^\circ C} \text{Orthorhombic} \xleftrightarrow{5^\circ C} \text{Tetragonal} \xleftrightarrow{130^\circ C} \text{Cubic}$$

The spontaneous polarization (P_s) occurs in the direction <111>, <110> and <001> in rhombohedral, orthorhombic and tetragonal structure, respectively. Therefore, $BaTiO_3$ shows strong temperature dependence of dielectric constant near their curie temperature which limits its application at high temperatures.

1.3.4.2 Calcium-Titanate ($CaTiO_3$)

It is a paraelectric material at room temperature with no interesting dielectric property in the pure form. Donor doping in $CaTiO_3$ gives rise to boundary layer effects with enhanced permittivity. Calcium titanate when doped with ≤ 0.75 mol % yttrium and sintered in N_2 atmosphere gives rise to anomalously high dielectric constants with relaxor behavior (Neirman *et al.*, 1984). It has distorted cubic structure (Kay *et al.*, 1957) and has an orthorhombic symmetry at room temperature. The structure becomes tetragonal at 600 °C, which changes to cubic at 1000 °C. The electrical conductivity of this compound at 130 °C, after exposing to oxidizing atmosphere, was found to be p-type (Cox *et al.*, 1967). $CaTiO_3$ can be converted to n-type semiconductor either by reduction at elevated temperature or by doping with donors (Neirman *et al.*, 1984).

1.3.4.3 Strontium Titanate ($SrTiO_3$)

At room temperature SrTiO3 is a centrosymmetric paraelectric material with a cubic perovskite structure. Below this temperature, it undergoes a ferroelectric transition with a very high dielectric constant (10^4). It has attracted much attention for its potential applications as substrate for epitaxial growth of high temperature

superconductor thin films (Chen *et al.*, 1988), in photolysis of water, as an oxygen sensor and in magneto-hydrodynamics operations (Butler *et al.*, 1981; Chang *et al.*, 1983), photo-chromic and cathode-chromic materials which are also used in memory devices, optical processors etc. (Phills *et al.*, 1969; Bernay *et al.*, 1981). It exhibits n-type conductivity due to formation of oxygen vacancies (Walters et al., 1967) and at room temperature it is cubic having a band gap of 3.2 eV (Mattheiss et al., 1972; Pertosa *et al.*, 1978) and is paraelectric (Mitsui *et al.*, 1961). Strontium titanate does not possess interesting properties in the pure form and at room temperature it is a cubic perovskite and a paraelectric (Parkash *et al.*, 1994). However, these properties can be modified by various substitutions which are important from device points of view. Doping in polycrystalline strontium titanate with several mol% bismuth or trivalent rare-earth ions has been found to result in relaxor behavior and high dielectric constant. For example, the room temperature dielectric constant for strontium titanate is ~300 whereas the dielectric constant is raised to ~18000 by doping with 0.75 to 1.0 mol% yttrium. Other important donor dopants are La^{3+}, Ce^{3+}, Sb^{5+} etc.

1.3.5 Applications of Perovskite Oxides

Perovskite oxides display a wide spectrum of interesting physical properties from both theoretical and technical application point of view. Colossal magnetoresistance, ferroelectricity, superconductivity, charge ordering, spin dependent transport, high thermo power and the interaction of structural, magnetic and transport properties are commonly observed features in this family. These compounds are used as sensors and catalyst electrodes in certain types of fuel cells and are potential candidates for memory devices and spintronics applications. The perovskites family includes many titanates which find broad application in various electro-ceramic applications, for examples, electronic, electro-optical and electromechanical applications of ceramics.

Many examples of perovskite compositions with various interesting properties can be found in the chemical literature. For example, many compounds like $La_{1-x}A_xMnO_{3+\delta}$ where A^{2+} is Ca, Sr, Ba or Pb, exhibits Colossal Magnetoresistance

(CMR). They have potential uses in data storage technologies, such as computer hard drives and floppy disks (Bhalla *et al.*, 2000).

Most of the perovskite oxides have high electrical resistivities, which make them useful as dielectrics. However, some of the perovskites behaves as good conductors and semi-conductors. A list of perovskite oxides with their dielectric constant is given in Table 1.1.

Table 1.1: Perovskites and their dielectric constant

Perovskites	**Dielectric Constant**
$BaTiO_3$ (ABO_3)	≥ 200 – 3000
$CaTiO_3$	≥ 100
$SrTiO_3$	≥ 320
Ba $(TiZr)O_3$	≥ 10,000
Pb $(Mg_{1/3}Nb_{2/3})O_3$	≥ 18,000
Pb $(Fe_{0.5}Nb_{0.5})O_3$	≥ 10^5
$CaCu_3Ti_4O_{12}$	≥ 10286
$CdCu_3Ti_4O_{12}$	≥ 409
$La_{2/3}Cu_3Ti_4O_{12}$	≥ 418
$Sm_{2/3}Cu_3Ti_4O_{12}$	≥ 1665
$Na_{1/2}La_{1/2}Cu_3Ti_4O_{12}$	≥ 3560
$Na_{1/2}Sm_{1/2}Cu_3Ti_4O_{12}$	≥ 1426
$Na_{1/2}Gd_{1/2}Cu_3Ti_4O_{12}$	≥ 1645
$Na_{1/2}Dy_{1/2}Cu_3Ti_4O_{12}$	≥ 1854
$Na_{1/2}Yb_{1/2}Cu_3Ti_4O_{12}$	≥ 2048
$LaCu_3Ti_3FeO_{12}$	≥ 44
$CaCu_3Ge_4O_{12}$	≥ 3

The rapid development of the microelectronic devices such as capacitors, resonators and filters increases the active demand of the high dielectric permittivity materials. Dielectric properties of these ceramics are useful for applications in capacitors and memory devices. Due to this trend, high dielectric constant materials such as barium titanate ($BaTiO_3$) and strontium titanate ($SrTiO_3$) and their isomorphs obtained by different substitutions are of prime importance in ceramic industries. A list of various application of perovskite is given in Table1.2.

Table 1.2: Few important applications of perovskite materials

Materials	**Applications**
$BaTiO_3$	Multilayer Capacitor, P.T.C. Thermistors
$SrTiO_3$	GBLC, P.T.C. Thermistors, Gas sensor
Pb $(Zr_xTi_{1-x})O_3$	Piezoelectric Transducer
$BaZrO_3$	Dielectric Resonator
(Pb, La) (Zr, Ti)O_3	Electro-optical modulator
$LiNbO_3$	Switches
$BaRuO_3$	Thick film Resistor
Pb $(Mg_{1/3}Nb_{2/3})O_3$	Electrostrictive Actuator
Ba (Pb, Bi)O_3 layered cuprates	Superconductor
$GdFeO_3$	Magnetic Bubble Memory
$YAlO_3$	Laser Host
(Ca, La) MnO_3	Ferromagnets
$LaCoO_3$	Refractory Electrodes
$KNbO_3$	Second Harmonic generator

1.4 $ACu_3Ti_4O_{12}$ TYPE OF MATERIALS

$ACu_3Ti_4O_{12}$ (ACTO) compounds based upon ABO_3 type perovskite-related structure exhibits high dielectric constant at room temperature**.** $ACu_3Ti_4O_{12}$ (where A = Ca, $Sm_{2/3}$, $Dy_{2/3}$, $Y_{2/3}$ and $Bi_{2/3}$) type perovskite crystallises into body centred cubic structure. The most studied perovskites, $CaCu_3Ti_4O_{12}$, possess high dielectric constant independent of frequency 10^2-10^6 Hz and temperature range 100-600 K (Subramanian *et al.*, 2000). Its static dielectric constant, that ultimately decides the degree of miniaturization, makes it valuable from device point of view. Additionally, many other perovskite materials e.g., $Bi_{2/3}Cu_3Ti_4O_{12}$ (BCTO), $Y_{2/3}Cu_3Ti_4O_{12}$ (YCTO) and $La_{2/3}Cu_3Ti_4O_{12}$ (LCTO), also exhibit high dielectric constant, showing similarity in dielectric behavior, i.e., all of these exhibit a Debye-like relaxation and their dielectric constants are nearly independent of frequency and temperature well below the relaxation frequency. $ACu_3Ti_4O_{12}$ type materials find many important applications in microelectronics and memory devices.

1.5 CALCIUM COPPER TITANATE ($CaCu_3Ti_4O_{12}$)

The need of finding alternative energy sources and their storage has undergone a phenomenal resurgence. New materials and novel engineering approaches are required to overcome the challenges facing the society to minimize its dependence on fossil fuel. The discovery of unusual high dielectric constant in $CaCu_3Ti_4O_{12}$ (CCTO) has opened a new field of research for material chemists. $CaCu_3Ti_4O_{12}$ exhibits high dielectric constant about 12,000 at 1 kHz which is nearly constant from room temperature to 300^{o}C and frequency independent in the range, 10^2-10^6 Hz. It does not show ferroelectric transition behavior due to its unusual dielectric property and non-linear varistor behavior (Li *et al.*, 2006).

Continuous efforts are being applied for investigation of miniaturized capacitor devices for large-scale energy storage systems as well as for advanced microelectronics, but neither the materials nor the engineering conditions have been solved satisfactorily till date. Researchers are attempting to reduce the size of all the communication devices as small and as light as possible. It is quite possible that CCTO can meet these requirements. There are some advantageous features of CCTO

compared to high dielectric constant ferroelectric materials for its applications to the miniaturization of electronic devices. However, the high dielectric loss is a significant obstacle in its experimentation. An ideal capacitor material must have high dielectric constant 10^2-10^6 and low dielectric loss (0.01-0.0001). The dielectric constant should not vary with the frequency in a large region and in addition, the dielectric material must show high thermal stability up to 500 ^oC. Some special properties of $CaCu_3Ti_4O_{12}$ that made it suitable for dielectric devices can be stated in brief as:

(i) It is non-ferroelectric with a very high dielectric constant. (Polycrystalline-10^4, Single Crystal- ~10^5, Depending on processing route ~10^2—10^6).

(ii) High dielectric loss (tan δ = dielectric loss/dielectric constant~0.1 or dissipation factor is related to loss of stored current)

(iii) No phase transition till ~ 800 ^oC.

(iv) Dielectric constant is stable between 100—600K and below 100K it drops suddenly to~100.

(v) Dielectric constant is stable in the low-frequency region, 10^2—10^5 Hz.

1.6 LITERAUTRE REVIEW

1.6.1 Advantage of $CaCu_3Ti_4O_{12}$ over $BaTiO_3$

Above 120^0C, Ti^{4+} in $BaTiO_3$ acquires full cubic symmetry. With decreasing temperature, Ti^{4+} is displaced toward one, then two and finally three oxygen anions and thus produces tetragonal around 130^oC, orthorhombic at 0^oC and rhombohedral at -90^oC respectively. The symmetry for Ti^{4+} in $CaCu_3Ti_4O_{12}$ is much lower than that in cubic $BaTiO_3$. It gradually reduces the possibility of a ferroelectric phase transition based on the displacement of Ti^{4+} from the centre of its octahedron. For example, the lack of a 4-fold axis in the Im_3 space group for $CaCu_3Ti_4O_{12}$ eliminates the possibility of a transition to a tetragonal ferroelectric structure. The Ti^{4+} cations could be displaced off-centric along its one 3-fold axis. However, this could not be a perfect ferroelectric transition, because the displacements would occur along four different directions. Thus, $CaCu_3Ti_4O_{12}$ has a complex perovskite-type structure where

polarizability and dielectric constant are enhanced by tension in Ti-O bonds where transition to a ferroelectric state is frustrated by the TiO_6 octahedra tilt structure that accommodates the square planar coordination of $Cu^{2+.}$

1.6.2 Crystal Structure of $CaCu_3Ti_4O_{12}$ (CCTO)

Crystal structure of CCTO was established with the help of XRD and neutron powder diffraction studies (Bochu *et al*., 1979; Ramirez *et al*., 2000). CCTO crystallizes in a perovskite structure of the type (A'A")(BO_3), where Ca^{2+} and Cu^{2+} ions share the A-site and Ti^{4+} at the B-site (Deschanvres *et al*., 1967; Bochu *et al*., 1979; Subramanian *et al*., 2000). The crystal structure of CCTO is cubic in the Im_3 (space group No. 204) (Adams *et al.*, 2006) with two formula units per unit cell because TiO_6 doublets are present in the structure (Ramirez *et al.*, 2000). The lattice parameter of this unit cell is 7.391 Å. The size difference between Ca^{2+} and Cu^{2+} causes the TiO_6 octahedra to undergo substantial tilting, leading to a body centred cubic lattice of space group Im_3 in which the Ti^{4+} ions occupy a centrosymmetric position in the octahedral sites. The angle of tilting is sufficiently large that the Cu^{2+} ions occupy an essentially square-planer environment (Adams *et al.*, 2006)**.** Each copper atom is bonded to four oxygen atoms and the large Ca-atoms are in corner and body centred position. The tilt angle of the TiO_6 octahedra is large enough (141°) to accommodate the local distortion which, in turn, would effectively rule out the real ferroelectric behavior (Nigro et al., 2006). In CCTO, the observed Ca-O distance is equal to 2.604 Å, which is, less than 2.72 Å, predicted from the ionic radii. Thus, the site is too small for the A^{2+} cation and the cation pushes out to expand the lattice which causes Ti-O bond under tension and increases the polarizability of the structure. The bond tension may increase or decrease if doped with suitable ions, having different ionic radii than Ca^{2+} and Ti^{4+} respectively. It results into change in polarizability value which, in turn, increases or the dielectric constant.

It has been found that CCTO structure remains centrosymmetric cubic even after doping up to very low temperatures. The structure of a unit cell of this composition is shown in Fig 1.8.

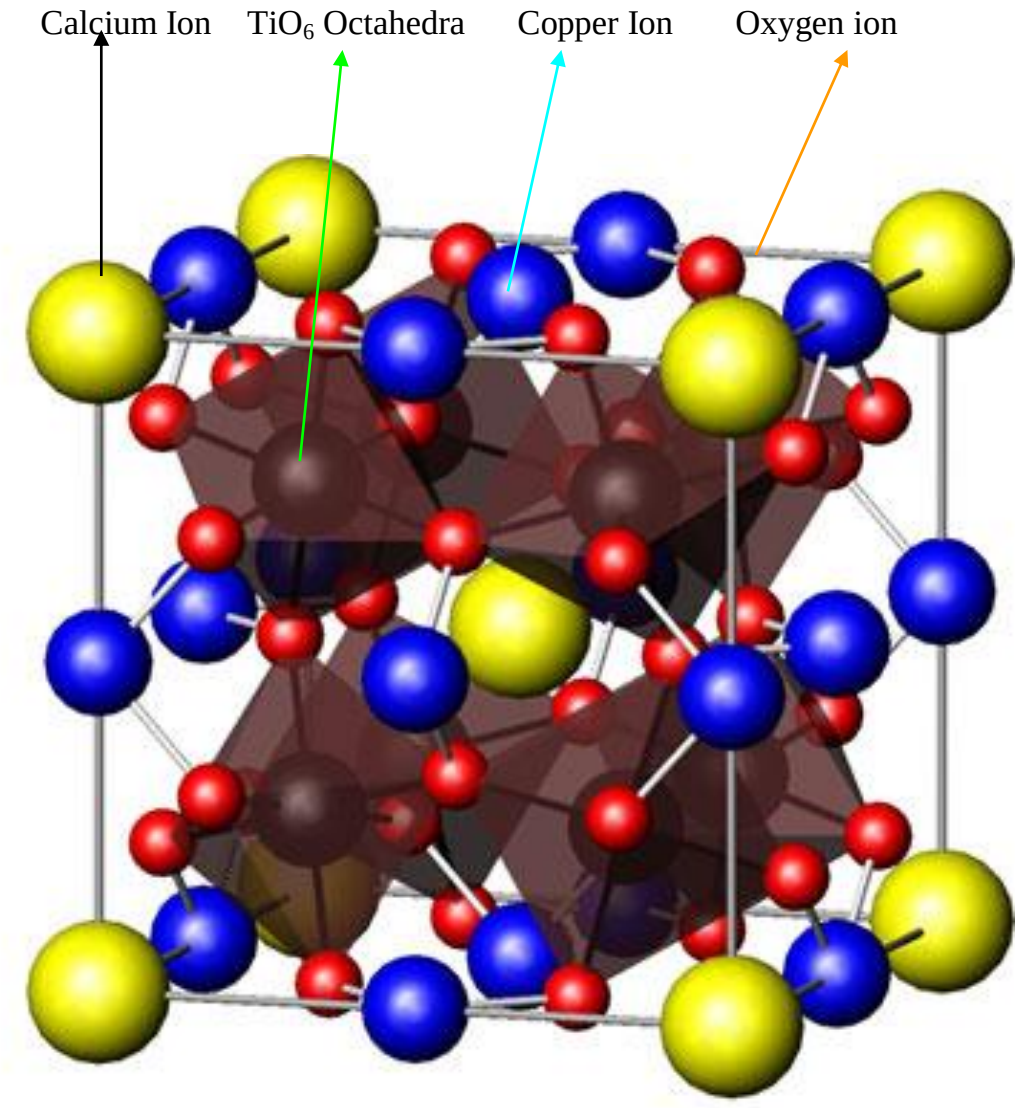

Figure 1.8: Crystal structure of $CaCu_3Ti_4O_{12}$ (Subramanian et al., 2000).

1.6.3 Origin of High Dielectric Constant in $CaCu_3Ti_4O_{12}$

$CaCu_3Ti_4O_{12}$ (CCTO) exhibits very high dielectric constant phenomena which is scientifically interesting and technologically intriguing. Therefore, the origin of large dielectric constant phenomena in $CaCu_3Ti_4O_{12}$ has attracted much attention. It is dependent on aspects interrelated to both intrinsic and extrinsic mechanisms. Several correlated to the origin of large dielectric response in CCTO are discussed below:

1.6.3.1 Intrinsic Mechanism: Atomic Structural Aspects

Intrinsic aspects of origin means the large dielectric response are from the relative cation shift that keeps intact the whole crystal structure. It may be inheritance of a perfectly stoichiometric, defect-free, single-domain crystal of $CaCu_3Ti_4O_{12}$. The CCTO structure is much more stressed than a regular ABO_3 type perovskite. The structure of unit cell is shown in Fig. 1.8, where the TiO_6 octahedra are tilted to produce a square planar environment for the Cu^{2+} ions. If Ti-O and Cu-O distances are 1.946 Å and 2.013 Å respectively, then the Ti-O octahedron is not distorted and for such regular CCTO crystal, the unit cell edge (a) and Ca-O bond distance must be found 7.349 and 2.581Å respectively. However, the Ca-O bond distance is much less than 2.72 Å, a prediction based on ionic radii (size effect). Thus in CCTO the Ca^{2+} ion is too small for it which pushes out to expand the lattice and Ti-O bonds get under tension. It increases the polarizability of the Ti-O octahedra. One may conclude that in CCTO, the dielectric constant and polarizability are enhanced by tension in Ti-O bonds. Subramanian *et al.* (2000) had interpreted the high dielectric constant response in terms of its intrinsic crystal structure, i.e., arising from the local dipole moments which are associated with off centre displacement of Ti ions, but the transition to a ferroelectric state is frustrated by the TiO_6 octahedral tilt being required to accommodate the Cu^{2+} square planar coordination. However, noticing the existence of high degree of twinning with small domains in the single crystal, they also suggest that these twin boundaries might act as the barrier layer capacitance, thus offering a possible extrinsic explanation for the observed giant dielectric property. From Raman scattering data obtained at different temperatures, Ramirez *et al.* (2000) obtained a temperature independent gap frequency equals to 28 meV, which is analogous to the thermal activation energy of dielectric constant of CCTO at low frequency. The indifferent relation between the gap frequency and the energy difference of two lattice sites suggests the possibility of highly polarizable relaxation modes in CCTO. Homes et al. also suggested that the variation in dielectric constant at low temperature may be due to relaxor behaviour which causes dynamic slowing down of dipolar fluctuations in nano-sized domains.

1.6.3.2 Extrinsic Mechanism: Microstructural aspects

The origin of extraordinary behavior of $CaCu_3Ti_4O_{12}$, in context of extrinsic aspects becomes easier to understand. The extrinsic contributions towards the dielectric response depend on microstructure and morphology the ceramic sample as well as domain boundaries and boundary layers developed during the processing step (Prakash *et al.*, 2008). These effects are the result of extrinsic domain walls and defect dipoles within the crystal. These mechanisms are thermally activated processes that can be frozen out at very low temperatures (Randall *et al.*, 1998). The factors are like domains and its domain boundaries in case of single crystal, grains and grain-boundaries in case of polycrystalline electrically heterogeneous materials, Electrode/sample contact effects, and interfacial polarization effects are mainly responsible for extrinsic contribution to high dielectric constant phenomena in CCTO.

1.6.3.2 (A) Single crystal of $CaCu_3Ti_4O_{12}$

In case of single crystal, the giant dielectric response in $CaCu_3Ti_4O_{12}$ is mainly due to the presence of boundary i.e. domains and its domain boundaries internally in the single crystal whereas grain boundaries for the polycrystalline $CaCu_3Ti_4O_{12}$. The insulating barrier layer of single crystals, locally planar twin boundaries, anti-phase and compositional-ordering domain boundaries were proposed to be the possibilities for the barrier layers (Fang *et al.*, 2007; Subramanian *et al.*, 2002).The recent concept of internal domains inside the grains has indeed solved this contradiction, which also strongly suggested that the origin of the giant dielectric response of $CaCu_3Ti_4O_{12}$ is related to the barrier layer mechanism. Fang *et al.*, (2007) and Ni *et al.*, (2007), had explained in context of internal domains inside grains. They proposed the possible existence of both domain boundaries and grain boundaries as the barrier layers to contribute the extraordinary dielectric response in $CaCu_3Ti_4O_{12}$ (Fang *et al.*, 2007). The discovery of the internal domains inside the grains of the polycrystalline $CaCu_3Ti_4O_{12}$ not only solves the contradictory explanation of the dielectric response between polycrystalline and single-crystal, but also justified the extrinsic effect of the enhancement of the dielectric response of $CaCu_3Ti_4O_{12}$.

1.6.3.2 (B) Internal barrier layer capacitor (IBLC) model

A barrier layer structure with semiconducting grains encircled by insulating layers was established to explain the very large capacitance behavior of both polycrystalline and single crystal $CaCu_3Ti_4O_{12}$ (Calvert *et al*., 2006; Chiodelli *et al.*, 2004). Internal barrier layer capacitance (IBLC) has been considered as the widely accepted mechanism to explain the observed giant dielectric response (Leret et al., 2007). The dielectric responses of such a structure are essentially characterized by interfacial polarization. For polycrystalline materials, the barrier layers are presumably located at the interface between the sample and contact, or at grain boundaries (Liu *et al*., 2005; Liu *et al.*, 2008). Sinclair *et al.*, (2002) used impedance spectroscopy to demonstrate that $CaCu_3Ti_4O_{12}$ ceramics are electrically heterogeneous, consisting of semiconducting grains (with dielectric constant <100) and insulating grain boundaries. A simplified equivalent circuit can be thus obtained, which consists of two parallel *RC* elements connected in series, one *RC* element, R_bC_b, representing the semiconducting grains (or bulk) and the other, $R_{gb}C_{gb}$, representing the insulating grain boundary regions (Hodge *et al.*, 1976). The equivalent circuit is shown in Fig. 1.9. In some cases, the semicircle corresponding to the grain (i.e. its electric response) is either missing or appears only partially at higher frequencies due to the limitation of the frequency range of the instrument. The study of impedance spectroscopy reveals the sample is electrically inhomogeneous in fact; the grains are semiconducting while the grain boundaries are insulating (Adams *et al.*, 2006). This study supports the "extrinsic" IBLC model as the origin of the high permittivity of $CaCu_3Ti_4O_{12}$ and also reconciled the "intrinsic" properties of $CaCu_3Ti_4O_{12}$. The barrier layers are supposed to be the grain-boundaries. The influence of average grain size on the electrical properties of $CaCu_3Ti_4O_{12}$ ceramics has been reported (Capsoni *et al.*, 2004). Extremely high grain boundary permittivity value of ~280000 was obtained in the large grained (~100-300 μm) ceramics, which provided further support for the extrinsic IBLC mechanism of the dielectric response in $CaCu_3Ti_4O_{12}$ ceramics.

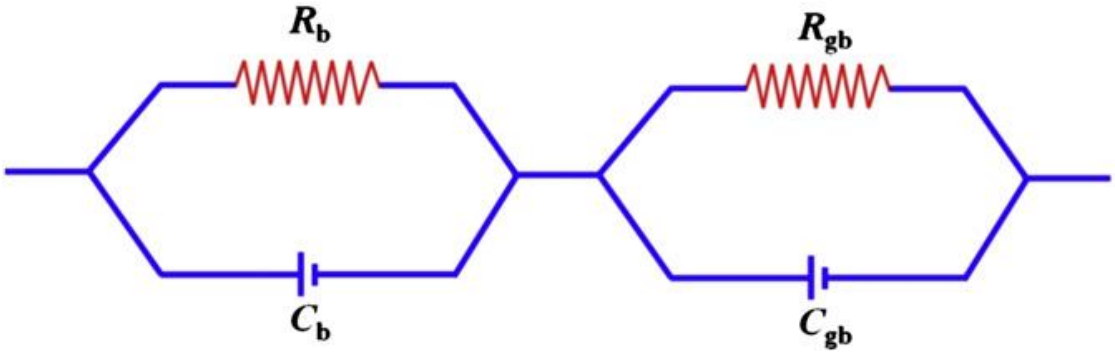

Figure 1.9: An equivalent circuit of the Cole-Cole plots.

1.6.3.2 (C) Electrode and sample contact effects

The high dielectric constant in $CaCu_3Ti_4O_{12}$ ceramic also originates from the electrode/sample contact effect. It depends on the surface resistivity of the sample. There will be no mobile space charges when the surface resistivity is as high as 1.2×10^8 Ω, so the dielectric properties of the sample are inert to the different metal electrodes and various sample thickness. Under this condition, the dielectric constant is near 2000 at frequency equal to 10 kHz at room temperature (Yang *et. al*., 2005). Measurement of the dielectric constant of the sample using platinum (Pt) electrode shows a significant change when the dielectric constant increased to 5000 at 10 kHz compared to silver (Ag) electrode (Lunkenheimer *et al*., 2004).

1.6.3.2 (D) Interfacial polarization effect: Maxwell-Wagner model

Interfacial polarization occurs in electrically inhomogeneous systems. When an electric current passes through interfaces between two different dielectric media, the surface charges pile up at the interfaces, due to their different conductivities, and it gives rise to a Debye-like relaxation process (Cole *et al.*, 1941; Cole *et al.*, 1942) under an external alternating voltage. A detected Debye-like relaxation response is, therefore, not necessarily the result of dipole relaxation in the system; sometimes it originates from the heterogeneity of the system (Pekhson *et al.*, 1987). For example, grains, grain boundaries or the electrodes and the sample having different conductivity can also produce the effect (Liu *et al.*, 2008). Conveniently, this effect can be described by the concept of the simplest equivalent circuit consisting of a

series of a network of three parallel RC elements. It has been widely used to account for dielectric relaxations in many heterogeneous materials (Liu *et al.*, 2008).

In summary, the giant dielectric constants have been variously attributed to:

i. the barrier layer capacitance arising at twin boundaries (Subramanian *et al.*, 2000),
ii. the difference in electrical properties between grain interiors and grain boundaries (Sinclair *et al.*, 2002; Liu *et al.*, 2008),
iii. the space charge accumulation at the interfaces between the sample and the electrode contacts (Lunkenheimer *et al.*, 2002; Lunkenheimer *et al.*, 2004),
iv. the polarizability contributions from lattice distortions (Chung *et al.*, 2005),
v. the differences in electrical properties due to internal domains (Fang *et al*., 2004),
vi. dipolar contributions from oxygen vacancies (Li *et al.*, 2004; Fang *et al.*, 2007),
vii. the role of Cu off-stoichiometry in modifying the polarization mechanisms (Fang *et al.*, 2007),
viii. the cation disorder induced planar defects and associated inhomogeneity (Zhu *et al.*, 2007) or
ix. the disorder of Ca/Cu substitution at a nanoscale level giving rise to electronic contribution from the degenerate e_g states of Cu occupying the Ca site contributing to the high dielectric constant (Wu *et al.*, 2005).

So far, several models have been proposed to explain the dielectric behavior and are quite controversial. But the mechanism for the giant dielectric constant of CCTO is still under question and investigators are trying their best to understand whether the giant dielectric constant is intrinsic within a perfect crystal or extrinsic one, where it originates from defects, in homogeneities, etc. To date, the IBLC explanation of extrinsic mechanism is comparatively widely accepted; however, none of the above approaches explains all the experimental findings satisfactorily.

1.6.4 How to Get High Dielectric Constant and Low Dielectric Loss in CCTO

Factors such as different synthetic routes, cationic substitutions at A-site, B-site, simultaneously at A-site and B-site as well as stoichiometric variations primarily influence the dielectric properties of CCTO. The dielectric constant (ε) and dielectric loss (tanδ) of CCTO are strongly dependent upon the processing conditions such as sintering temperature, sintering time, cooling rate and partial pressure of sintering atmosphere.

1.6.4.1 By Using Different Synthetic Routes

Liu *et al.* (2008) had reported synthesis of fine crystalline CCTO powder with a homogeneous distribution grains in the range 0.4 - 1.5 μm by using wet chemical method at relatively lower temperatures and a shorter reaction time. Jin *et al.* (2007) used the nano ultrafine powders for the preparation of CCTO ceramic by the sol-gel method involving citrate auto-ignition.

Hutagalung *et al.* (2008) synthesized CCTO by microwave assisted solid state reaction technique. This involved the preparation of raw materials, mixing and milling, calcinations, pellet forming and sintering process. Conventional furnace and microwave assisted sintering processes were employed in order to improve phase structure, morphology and dielectric properties of CCTO ceramics. Surface and fracture SEM analysis showed that microwave assisted sintered CCTO produced better densification and more uniform grain size compared to conventional sintered sample. Thomas *et al.*, (2008) synthesized nanoparticles of CCTO from precursor route giving nanoparticles of the CCTO with the crystallite size varying from 30-200nm below temperature 680 $^{\circ}$C. The required optimum temperature was determined by the exothermic thermal decomposition of an oxalate precursor $CaCu_3(TiO)_4(C_2O_4)_8.9H_2O$. The wet chemical analysis confirmed the single phase formation of the oxalate precursor complex. The powders derived from the oxalate precursor route have excellent sintering ability resulting in high density ceramics giving high dielectric constant up to 40000 (1 kHz) at 25 $^{\circ}$C accompanied by low dielectric loss (< 0.07). Masingboon *et al.* (2008) have synthesized nano-sized

powders of CCTO by polymerized complex method by its calcination at 600, 700 and 800 °C in air for 8 h. The particle size of powder was found to be in the range 30-100 nm. SEM micrographs of the sintered ceramics showed the grain size of 10-15 µm and the samples exhibit the giant dielectric constant in the range 10000-20000. It is found that dielectric constant is independent of frequency and weakly dependent on temperature. Maxwell-Wagner model is used to explain the giant dielectric constant present in these materials.

Rossignol *et al.* (2009) had reported synthesis and dielectric properties of CCTO based ceramics and thick films (~ 50 µm) prepared from powders synthesized by a chemical method and they have compared characteristics of pellets and thick films. The pellets exhibit high values of dielectric permittivity (ε ~ 1.4 x 105) and relatively small dielectric losses (tan δ ~ 0.16) at 1 kHz and at room temperature. Zhu *et al.* (2007) prepared CCTO by oxalate co-precipitation method which is done at lower temperature and within a shorter reaction time than that for conventional solid state reaction. Smith *et al.* (2009) synthesized low loss colossal dielectric CCTO by an anion substitution route in which oxygen was substituted partially by fluorine. It reduced the dielectric loss but retained a high dielectric constant with temperature independent behaviour from 25 to 200 °C. The ceramic, $CaCu_3Ti_4O_{11.7}F_{0.3}$, exhibited a giant dielectric constant over 6000 and low dielectric loss below 0.075 at 100 kHz within a temperature range, 25-200 °C. The fluorine analysis confirmed the presence of fluorine in all samples measured.

1.6.4.2 Processing Conditions

Prakash *et. al.* (2007) described a remarkable change in the microstructure in which some grains show abnormal growth and Cu-rich smaller grains occupy the intermittent regions. Further increase in sintering duration to 15 h increased the dielectric constant value to more than 24,000. Density difference and grain size do not have a strong effect to improve the dielectric constant. When $CaCu_3Ti_4O_{12}$ sample was annealed in a flow of argon at 1000 °C, the dielectric constant was close to one million at room temperature. Kwon et al. (2009) studied the structure–property relationship of the $CaCu_3Ti_4O_{12}$ ceramics prepared by conventional solid-state method for different sintering duration. X-ray diffraction patterns of the tenorite CuO and

cuprite Cu_2O secondary phases, found on the unpolished and polished surfaces of $CaCu_3Ti_4O_{12}$, were explained by the reduction/reoxidation reaction as a function of sintering time. Based on the microstructures, grain growth of $CaCu_3Ti_4O_{12}$ continued from 0.5 to 4 h sintering while the further growth was limited to the small-sized grains after 8 h sintering. The changes in dielectric constant and tan δ concerning the secondary phases and the microstructures of the different sintering hours were discussed.

Singh *et al.* (2011) synthesized nano-structured $CaCu_{2.90}Zn_{0.10}Ti_4O_{12}$ (CCZTO) sintered at 950 °C for 6h, 8h and 12h in air ceramic by semi-wet route. The pellets exhibit high dielectric constant of 1.35×10^4 at 1 kHz. It was observed that the grain size significantly increased with an increase in sintering duration. Dielectric constant also increases with increasing sintering time and dielectric loss decreases. It is suggested that the longer sintering time may lead to more defect structures. The size of a particle increases with increasing sintering time which is mainly due to formation of large size particles as a result of loss of grain boundaries of small size particles. These changes lead to stability of the large size particles due to loss in grain boundary.

1.6.4.3 Substitutions Effects on CCTO Electro-ceramic

Parkash *et al.* (2006) examined the effect of La^{3+} doping on Ca^{2+} site in $CaCu_3Ti_4O_{12}$ (CCTO) using the sample synthesized by conventional solid state reaction route. A remarkable decrease in grain size from 50 μm to 3-5 μm was observed in La^{3+}substitution and the dielectric constant of $CaCu_3Ti_4O_{12}$ was found to decrease drastically on La^{3+} doping. The impedance spectroscopy showed that La^{3+} substitution at the Ca^{2+} site resulted in an increase in the resistance of the grains and a decrease in the grain boundary resistance, consequently, a decrease in the grain boundary internal barrier layer effect.

Mandal *et al.* (2009) synthesized $Ca_{1-x}La_xCu_3Ti_{4-x}Co_xO_{12}$ (x =0.10, 0.20 and 0.30) using metal nitrate solutions and solid TiO_2 powder. The dielectric constant and dielectric loss of x = 0.30 composition was found to be 2000 and 0.50, respectively at room temperature (1 kHz). Dielectric constant for the composition x = 0.30 is higher

than the other two compositions over the measured frequency range. AC conductivity of $Ca_{1-x}La_xCu_3Ti_{4-x}Co_xO_{12}$ sample increases with increasing temperature and shows the semiconducting behavior of the materials. Cai et al. (2007) showed a remarkable effect of Mn doping on the dielectric and nonlinear electric properties of $CaCu_3Ti_4O_{12}$ ceramics. The Mn doping at only 2.5% can suppress the dielectric permittivity in $CaCu_3Ti_4O_{12}$ up to two orders of magnitude from 10^4 to $10^2$and the non-linear varistor characteristics disappear completely. It is due to the lowering of the height of potential barrier at the grain boundary as well as charge compensation for the conduction electrons caused by Mn doping. Kwon et al. (2008) studied the substitution of Cr_2O_3 on the Ti site in terms of its effect on the dielectric properties in the doping level ranging from 0.1 to 1.0%. The permittivity and dielectric loss of 1% Cr_2O_3 doped $CaCu_3Ti_4O_{12}$ were improved with ε_r~19,000 and tan δ ~0.049 at 1 kHz. Also, 1% Cr_2O_3 doping was effective in maintaining the high ε_r up to 150 V. From these results; it can be inferred that Cr_2O_3 doping is an efficient method to achieve a high-ε and low loss value. Mu *et al.* (2009) studied the effect of Fe^{3+} substituted $CaCu_3Ti_{4-x}Fe_xO_{12}$ (CCTFO, $0 \leq x \leq 0.2$) ceramics prepared by solid-state reaction. The dielectric spectroscopic studies disclosed the presence of multiple relaxation processes responsible for the origin of dielectric phenomena in $CaCu_3Ti_{4-x}Fe_xO_{12}$ ceramics. The resistivity of grains and grain boundaries got increased while dielectric constant decreased dramatically in the frequency range of 1 kHz to 1MHz with increasing iron content $x \leq 0.2$. Shao *et al.* (2007) examined the effect of La at Cu site with the nominal compositions of $CaCu_{3-x}La_{2x/3}Ti_4O_{12}$. He got that $CaCu_{2.9}La_{0.2/3}Ti_4O_{12}$ ceramic sintered at 1050 $^{\circ}$C for 20 h exhibited the high dielectric constant, ε~ 7500 with weak frequency dependence below 1 MHz. It also exhibited low dielectric loss lesser than 0.05 in the frequency range of 120 Hz–200 kHz with the minimum value, tan δ ~ 0.012 at 20 kHz. The presence of CaTiO3 as a secondary phase is due to Cu deficiency and La doping plays the important role in the observed excellent dielectric properties in $CaCu_{3-x}La_{2x/3}Ti_4O_{12}$ ceramics.

Choi *et al.* (2007) studied the substitution effect of Al-doped $CaCu_3Ti_{4-x}Al_xO_{12}$-$x/2$ (x = 0.0-0.1) ceramics and found that the dielectric loss reduces remarkably, maintaining the high dielectric constant value. The tan δ was below 0.06 for the x = 0.06 over the frequency range of 10^2–10^4 Hz, with ε~ 41000 at 10 kHz.

Impedance spectra indicated that Al doping increases the resistivity of the grain boundary by an order of magnitude. The improvement in the dielectric loss in Al-doped CCTO was attributed to the enhanced grain boundary resistivity. Hutagalung *et al.* (2009) studied the effect of zinc doping on the dielectric properties $CaCu_3Ti_4O_{12}$ at low frequencies and observed that the dielectric constant had a minimum value at 1.5 mol% of Zn. The minimum dielectric loss was observed at 5 mol% Zn at 1 kHz. The value of dielectric loss decreases from 30% (un-doped) to a minimum value of 18% at 5 mol% Zn dopant. Sen *et al.* (2010) report the effect of vanadium doping on the dielectric and electrical properties of giant dielectric material $CaCu_3Ti_4O_{12}$ (CCTO). The X-ray photoelectron spectroscopic studies confirmed the replacement of Ti^{4+} by V^{4+}at its lattice site. The grain boundary resistivity was found to decrease monotonically with the increase of V doping percentages as revealed by impedance spectroscopic measurement and furthermore the grain size was determined to follow the similar trend. Li *et al.* (2008) reported the effects of the Mg doping on the dielectric properties of $CaCu_3Ti_4O_{12}$ in the frequency range, 200 Hz–200 kHz and in the temperature range, 58–473 K. They found that the incorporations of Mg^{2+} results in increases in the dielectric constant by 12–20% and a decrease in the dielectric loss by 41–64% with the minimum value 0.042 for $CaCu_{2.7}Mg_{0.3}Ti_4O_{12}$ at room temperature and 1 kHz. The x-ray photoemission spectroscopy measurements reveal that the content of Cu^{3+} increases with the increasing concentration of Mg^{2+}. Zheng *et al.* (2012) prepared pure and chromium-doped CCTO ($CaCu_3Ti_4O_{12}$) ceramics and observed the dielectric constant value as high as 20,000 (at 1 kHz) when dopant concentration is 3%. The obtained activation energy associated with the electrical relaxation determined from the electric modulus spectra was 0.50–0.60 eV, which was very close to the value of the activation energy for dc conductivity (0.50 ± 0.05 eV). These results suggest that the movement of oxygen vacancies at the grain boundaries is responsible for both the conduction and relaxation processes.

1.7 AIM OF THE PRESENT STUDY

A continuous demand for miniaturization of electronic devices such as cell phones, digital cameras, notebook, computers, TV, etc has created a keen interest to explore new capacitor materials exhibiting high dielectric constant with low loss for application to microelectronics, microwave, memory and capacitance based energy storage devices.

CCTO can meet both these requirements due to very high thermal stability and colossal dielectric constant, stable between 100—600K in the low frequency region 10^2-10^5 Hz. In fact, the complex perovskite $ACu_3Ti_4O_{12}$ (A = Ca, $Bi_{2/3}$, $Y_{2/3}$) possess high dielectric constant. All of them could be a promising candidate to replace relaxors as dielectrics in DRAM, MLCCs, super capacitors and other memory devices. Their smaller capacitive components lead to miniaturization of electronic devices with efficient performance. Such materials could be technically significant for introducing the state of art in semiconductor integrated circuits (ICs) owing to their high reliability, high integration potential, good dielectric properties and excellent thermal conductivity as their thermal expansion coefficient close to silicon. It is desirable to investigate systematically new CCTO like materials possessing temperature independent high dielectric constant and low dielectric loss with good thermal stability. $Y_{2/3}Cu_3Ti_4O_{12}$ (YCTO) is very much similar to CCTO and has the same crystal structure.

In the present exploratory work, an attempt has been made to synthesize undoped and a few doped samples of $Y_{2/3}Cu_3Ti_4O_{12}$ (YCTO) material by semi-wet auto-combustion citrate-nitrate route and then characterization. In semi wet route, the solution of nitrates of all ions except titanium is used in solid form as TiO_2. By using this method, these samples can be synthesized at a relatively lower temperature and short duration. The mixing process is performed in a sol state. Each constituent ion is uniformly dispersed in the resulting mixture after removing organic matter by heating in air. As per present literature, a few works have been reported on YCTO ceramic. Liang et al. (2012) have reported the dielectric loss (tan δ) values of YCTO ceramic in kHz range only which was prepared via solid-state reaction method while Li et al. (2015) has discussed the phase formation with enhanced dielectric response of YCTO

ceramics derived from Sol–Gel process. Detail studies on YCTO system regarding methods of processing, sintering times, sintering temperatures, doping schemes as well as nature of dopants and their stoichiometric variations and its impact on various material properties has yet to be disclosed.

1. This work focuses on the study of the synthesis of undoped and a few doped samples of $Y_{2/3}Cu_3Ti_4O_{12}$ (YCTO) and their characterization.

2. It discusses the effect of different cationic substitutions such as Zn^{2+} or Mg^{2+} at Cu site, Fe^{3+} at Ti^{4+} site, $La^{3+}$and Bi^{3+} on Y^{3+} site in $Y_{2/3}Cu_3Ti_4O_{12}$ on the dielectric properties and electrical behavior as a function of temperature and frequency.

3. The microstructure of the different ceramics will also be studied along with separation of grains and grain boundaries contributions to the electrical and dielectric properties at different temperatures and frequencies.

4. The effects of sintering temperature and sintering duration and processing routes like conventional solid-state method, semi-wet method or ball-mill route etc. will be studied so that one can obtain a good quality of $Y_{2/3}Cu_3Ti_4O_{12}$ electro-ceramic.

5. In addition, an effort will be made to get high dielectric constant and low dielectric loss YCTO ceramic suitable for use as capacitor material showing high thermal stability and independent on frequency.

With these objectives mentioned, the present exploratory research work is to synthesize the following YCTO and its isomorphs would be carried out in the following steps:

1. Synthesis the following samples :
   (i)$Y_{2/3}Cu_3Ti_4O_{12}$ (YCTO)
   (ii) $Y_{1/3}La_{1/3}Cu_3Ti_4O_{12}$ (YLCTO)
   (iii) $Y_{2/3}Cu_{3-x}Zn_xTi_4O_{12}$ (YCZTO) (x = 0.10, 0.20, 0.30)
   (iv) $Y_{2/3}Cu_3Ti_{4-x}Fe_xO_{12}$ (YCTFO) (x = 0.05, 0.10, 0.15, 0.20)
2. Characterizations of sample were carried out by different physiochemical methods by the following sequential steps:

i. DTA/TGA technique to determine the ideal temperature of calcination and sintering.
ii. Study the crystal structure and single phase formation of the ceramic compositions using X-ray powder diffraction.
iii. Determination of density and porosity of sintered materials.
iv. Study of the surface morphology using Scanning Electron Microscopy (SEM).
v. To study the purity and stoichiometry of each of grain and grain-boundary region by elemental analysis by will be assessed by the energy dispersive X-ray spectroscopy (EDX).
vi. Determination of particle size by Transmission Electron Microscopy (TEM).
vii. Investigation of dielectric properties as a function of temperature as well as frequency.
viii. In addition, a correlation between dielectric behavior and those of microstructure and defect structure will also be established.
ix. Rationalization of dielectric properties by impedance, modulus and admittance spectroscopic studies.
x. Study of AC conductivity as a function of temperature and frequency to investigate the mechanism of conduction.

These ceramics will be characterized by different physiochemical techniques. TG/DTA will be utilized to determine calcination temperature of the precursor, the powder X-ray diffraction will be recorded to study the crystal structure and single phase formation of the ceramic. Scanning electron micrographs of the ceramics will be recorded to study the surface morphology and transmission electron micrographs will be obtained to determine their particle size. The purity and stoichiometry of each of grain and the grain-boundary region will be assessed by the energy dispersive X-ray studies. In order to obtain high dielectric constant and low dielectric loss ceramic the dielectric and electrical properties will be studied as a function of temperature as well as frequency. In addition, a correlation between dielectric behavior and those of microstructure and defect structure will also be established.